

General Disclaimer

One or more of the Following Statements may affect this Document

- This document has been reproduced from the best copy furnished by the organizational source. It is being released in the interest of making available as much information as possible.
- This document may contain data, which exceeds the sheet parameters. It was furnished in this condition by the organizational source and is the best copy available.
- This document may contain tone-on-tone or color graphs, charts and/or pictures, which have been reproduced in black and white.
- This document is paginated as submitted by the original source.
- Portions of this document are not fully legible due to the historical nature of some of the material. However, it is the best reproduction available from the original submission.

Final Report to the
NASA Langley Research Center
Grant NSG-1612

May 1980

Department of Engineering and Applied Science
Yale University, New Haven, CT 06520

(NASA-CR-163217) STUDY OF EXPERIMENTS ON
CONDENSATION OF NITROGEN BY HOMOGENEOUS
NUCLEATION AT STATES MODELLING THOSE ON THE
NATIONAL TRANSONIC FACILITY Final Report
(Yale Univ., New Haven, Conn.) 58 p

N80-25294

Unclas
G3/02 22392



Yale University *New Haven, Connecticut 06520*

DEPARTMENT OF ENGINEERING
AND APPLIED SCIENCE

Mason Laboratory
9 Hillhouse Avenue
(203) 436-3563

May 1980

Final Report to the
NASA Langley Research Center
on Grant NSG-1612

STUDY OF EXPERIMENTS ON CONDENSATION OF NITROGEN
BY HOMOGENEOUS NUCLEATION AT STATES MODELLING
THOSE OF THE NATIONAL TRANSONIC FACILITY.

Submitted by

Peter P. Wegener

Peter P. Wegener

Principal Investigator

OUTLINE

	page
1) INTRODUCTION AND OVERVIEW	1
2) NITROGEN CONDENSATION EXPERIMENTS	5
a) Experimental Results	5
b) Discussion of Results	10
3) STUDY OF PROPOSED CONDENSATION EXPERIMENTS	15
4) ACKNOWLEDGMENT	21

TABLES AND FIGURES

APPENDIX: Isentropic Expansion of Nitrogen using Berthelot's
Equation of State.

1) INTRODUCTION AND OVERVIEW

A research proposal "STUDY OF EXPERIMENTS ON CONDENSATION OF NITROGEN BY HOMOGENEOUS NUCLEATION AT STATES MODELLING THOSE OF THE NATIONAL TRANSONIC FACILITY" was submitted to NASA-Langley dated 1 January 1979 to cover a period of 1 April to 21 December 1979. Funding was received on 4 June 1979 to cover a period of 15 May 1979 to 14 February 1980 with a later extension without additional funds to 30 April 1980. The final report at hand covers the work done under the listed grant. For past history and motivation we refer to the text and references given in the Proposal. A cryogenic wind tunnel is based on the twofold idea[†] of lowering drive power and increasing Reynolds number by operating with nitrogen near its boiling point. There are two possible types of condensation problems involved in this mode of wind tunnel operation. They concern the expansion from the nozzle supply to the test section at relatively low cooling rates, and secondly the expansion around models in the test section. This secondary expansion involves higher cooling rates and shorter time scales. In addition to these two condensation problems it is not certain what purity of nitrogen can be achieved in a large facility. Therefore one cannot rule out condensation processes other than those of homogeneous nucleation. In sum, the data on N₂-condensation of previous work shown in Figure 1 (for references see the Proposal) in

[†] E.C. Polhamus, R.A. Kilgore, J.B. Adcock and E.J. Ray, "The Langley Cryogenic High Reynolds Number Wind-Tunnel Program", Astron. & Aeron., October 1974.

conjunction with two typical isentropes may well be insufficient for accurate prediction of operating conditions for the Langley facility.

To repeat in part from the Proposal.

- (a) Expected supercooling at higher pressures is not well known (supply pressure of 1 to 10 atm for a Mach number range of $-0.7 < M < 2$ are anticipated for the transonic facility).
- (b) The experimentally available range of the cooling rate effect on supercooling is not sufficiently wide to cover the needs of the transonic facility. Expansion rate effects in the free stream and the higher rates around models and their components must be understood.
- (c) The effects of purity on condensation of the nitrogen used for tunnel operation is not understood. Heterogeneous and binary (or heteromolecular) effects must be studied to understand nucleation in a practical situation for nitrogen available in large amounts.

The question of what impurity level can be tolerated may well prove to be one overriding importance for the operation of the transonic wind tunnel facility in the supersaturated regime. There is clear evidence that nitrogen expansions can be nucleated heterogeneously resulting in little or insignificant supercooling. Heterogeneous nucleation has been demonstrated in a qualitative manner for other gases and in a semi-quantitative way here at Yale[†] for the

[†] For references see the Proposal.

condensation of ethyl alcohol and also for sulfur hexafluoride, both present in non-condensing carrier gases.

The study performed under this grant addressed itself to some of the points raised. The summer of 1979 was used to compute isentropic expansions of nitrogen based on real gas (equilibrium) properties. The Berthelot equation of state was chosen as the thermal equation of state, and it was integrated together with caloric data on N_2 at zero pressure taken from the literature. This procedure yielded the real gas isentropes. The Berthelot equation is found to be a substantial improvement over van der Waal's work in predicting the state of a real gas in the range of pressures of interest here. The more complicated equations such as that proposed by Beattie and Bridgman which are useful at much higher pressures can thus be avoided. The results of this calculation are given in the Appendix. It became clear that real gas effects are in fact negligible in the range of interest given, provided no condensation appears.

In parallel, a study was carried out to determine design parameters of a small wind tunnel operated much like that used for previous condensation studies on sulfur hexafluoride in argon[†] and argon in helium.^{††} A few of the results of more extensive studies are discussed in Section 3 of this final report. An experimental setup such as shown schematically

† B.J.C. Wu, P.P. Wegener and G.D. Stein, J. Chem. Phys. 68, 308 (1978).
B.J.C. Wu, and G.A. Laguna, J. Chem. Phys. 71, 2991 (1979).

†† B.J.C. Wu, P.P. Wegener and G.D. Stein, J. Chem. Phys. 69, 1776 (1978).

in Figure 2 is envisioned. The gas supply consists of bottled N_2 which is passed via a sonic orifice valve and additional control valves through a heat exchanger embedded in an insulated vessel filled with liquid nitrogen. In this fashion supply temperatures down to about 100 K can be achieved. The once-through system operates continuously via a plenum chamber and two existing Stokes Microvac Model 412-H pumps operating in parallel at a combined displacement of 600 CFM. Instrumentation and methods of observing condensation are in principle along the lines of those to be discussed in the next Section of this report.

The study revealed that it would be difficult to duplicate the low cooling rate of the Langley Transonic Facility as measured from the supply to the test section. However, a wide range of cooling rates as typically to be expected around models can readily be produced in a range of nozzles operated to duplicate the thermodynamic states of the full-scale facility. The points raised initially in this Section could then be answered in a systematic study.[†]

Finally, a few experiments on condensation of nitrogen using existing equipment were suggested in the proposal for late summer of 1979.^{††} However, in our continuing contacts with Dr. Robert M. Hall of NASA-Langley -- the technical monitor of our work -- it became apparent that changes in the original plans might be useful as NASA's interests change. For one, the

† In a separate study at our laboratory for the NASA Ames Laboratory it becomes apparent that our theoretical understanding of binary, heteromolecular and heterogeneous nucleation is far from satisfactory. This fact suggests an empirical approach to solve practical engineering problems at this time.

†† These experiments cover the lowest cooling rates ever achieved in steady supersonic flow used for condensation studies of nitrogen.

primary condensation interest appeared increasingly to focus on the expansion around models. No chance could be taken to operate the test section at a supersaturated state. Therefore it was decided to operate at Yale as part of the subject grant a more extensive series of nitrogen condensation experiments. In turn consumables (primarily gaseous and liquid nitrogen), small parts, etc. were used in excess of the budgeted amounts. Moreover more manpower than originally planned was needed to prepare the condensation setup. The actual expenditures exceeded the budget and they will be submitted separately.

The results of these experiments covered at least a part of the range of interest to the Langley facility. In particular the cooling rates were somewhat lower than those of previous experiments (Figure 1) and they resulted in a smaller supersaturation before condensation set in.[†] Moreover, it is believed that our method of detection of the onset of condensation by light scattering is more sensitive than the instrumental approaches of previous work. Prior to our experiments nitrogen condensation was observed by pressure measurements. Thus our data may lead to an earlier detection of phase change on a given isentrope. This work will be discussed in the next section.

2) NITROGEN CONDENSATION EXPERIMENTS

a) Experimental Results

The experiments to be described next covered the range of states in the vicinity of Isentrope #2 in Figure 1. The cooling rates were of the order of 0.1 C/ μ s. Apparatus close to that shown in Figure 2 was used, however the light beam of a Helium/Cadmium laser (442 nm) was passed

[†] See footnote on previous page. This statement applies to the pressure range of our experiments.

beyond the nozzle exit via a first surface mirror and a prism at right angles to the flow direction. In turn the photomultiplier was mounted at 90° to the incident light beam perpendicular to the flow direction. Bottled nitrogen of purity 99.998% was passed via a sonic orifice and a control valve through three separate copper coils embedded in an insulated heat exchanger filled with liquid nitrogen.[†] The cooled nitrogen gas entered the supply section as shown in Figure 2 and the double walled supply was cooled with liquid nitrogen. The arrangement is shown in Figure 3 with details of the laser seen in Figure 4. The supply temperature was measured by a thermocouple versus a cold junction at 0°C . A Wallace and Tiernan aneroid pressure gauge in parallel with a Baratron were used to measure the supply pressure. Previously it had been shown that the supply temperature remains constant across the supply chamber of the wind tunnel. The range of temperatures covered was $107 < T_0 < 124^\circ\text{K}$. Higher temperatures were difficult to achieve because individual coils could not be removed from the circuit without extensive redesign.

The nozzle used was designated as Nozzle B as listed in Table 1. It is moreover shown full scale in Figure 5. A free jet issued into an open chamber at the nozzle exit (Figure 2) and the jet could be observed through two windows. Several pressure taps connected to a single tube are located 3 mm upstream from the nozzle exit (Figure 5). This pressure is designated as p_e and it is measured with a Baratron pressure gauge which was calibrated with a Wallace and Tiernan mercury precision manometer. Finally, the pressure in the plenum chamber was kept at or below the nozzle exit pressure.

[†] The N_2 was Grade P.P. ("prepurified") with max. moisture 3 parts/million, max. O_2 5 parts/million (Linde Corp.).

The nozzle was first calibrated by measuring the exit pressure as a function of the supply pressure for a room temperature supply. The results of this calibration are shown in Figure 6 together with the computed effective area ratio. We note the Reynolds number effect with decreasing exit pressure ratio (i.e. higher Mach numbers) at higher supply pressures. At $p_0 = 1$ atm, the Reynolds number per unit length at the nozzle exit is about $Re/\ell \approx 10^7 \text{ m}^{-1}$ at $M \approx 2.5$. Unfortunately a similar calibration does not exist for nitrogen with a "cold" supply because of a malfunction of the pressure connection that was subjected to the low temperatures.

The condensation experiments were conducted with continuous flow. Test section and heat exchanger were precooled by passing a low flow rate through the apparatus. The supply temperature was varied by altering the mass flow rate in the heat exchanger by a variation of the supply pressure.[†] After the desired temperature was obtained, the supply pressure was raised until a light scattering response was barely perceived above the signal given by the background light and the electronic noise. Lowering the pressure led again to a disappearance of light scattering and repeated pressure changes up and down provided a check of the operation. The voltage from the photomultiplier, the supply pressure, Baratron output and the supply temperature were recorded on Hewlett-Packard strip chart recorders and simultaneously read on digital voltmeters.

[†] Independent temperature control by separate operation of parts of the heat exchanger will be essential in future experiments.

A series of condensation experiments as described were performed from 28 November to 2 December 1979. Of this series 17 reliable data points on the onset of condensation of nitrogen in Nozzle B (Table 1, Figures 5 and 6) were obtained. The raw data and derived results of these experiments are listed in Table 2 as explained in the legend of Table 3. The data reduction method will also become apparent from Table 3. The main points of the procedure are as follows. For each experiment column (1) at a measured value of steady flow with p_0 (2), and T_0 (3), (4), the onset of condensation was noted at the nozzle exit by a barely perceptible light scattering increase above the background signal. Because of the unfortunate absence of a "cold" calibration, two limiting values of the corresponding onset state of condensation were determined from the raw data. One limit is given by assuming the absence of viscous effects, i.e. flow without a boundary layer. The other limit is obtained by relying on the room temperature nozzle calibration of Figure 6. Clearly the actual value on a given isentrope will be found somewhere in between the two extremes (note later discussion). The onset of condensation in these experiments at $M \approx 2.5$ does not lead to thermal choking permitting the straightforward calculation of states on an isentrope without regard to heat addition by condensation whose value is much below the critical one. Finally, all results of Table 2 were computed by treating nitrogen as a thermally and calorically perfect gas.[†]

The experimental results of Table 2 are given in Figure 7. The

[†] The justification for this procedure is discussed in the Appendix.

saturation vapor pressure, $p_{\infty}(T)$ with respect to a flat surface[†] is also plotted. Seven sample isentropes are shown for supply pressures of 0.5 to 9 atm at different supply temperatures. Mach numbers are marked off on these isentropes. Experiment #32 at $T_0 = 129K$ and $p_0 = 1.5$ atm is also indicated by an isentrope with the limiting condensation states marked off. All other experiments are indicated by their number at the supply state and a short isentrope that brackets the onset of condensation within the two assumptions previously given. The mean value of the limiting experimental results is shown by a dashed line which indicates an adiabatic supercooling^{††} of roughly $10^{\circ}C$ shifted in parallel to the vapor pressure curve.

The cooling rate will next be calculated. With relatively small changes of the Mach number, flow speed, etc. between saturation and condensation, it is reasonable to define an average speed between these two states. The state at saturation can be roughly located in the nozzle based on the effective area distribution $A/A^* = f(x)$ from the previous nozzle calibrations.^{†††} The onset of condensation is, of course, found at the nozzle exit in view of our experimental method. Choosing the mean value curve of Figure 7 for the onset of condensation, the results shown in the upper half of Table 4 emerge. We note that the adiabatic supercooling, ΔT_{ad} , has the narrow range of

† National Bureau of Standards, Circular 564, (1955).

†† The adiabatic supercooling, ΔT_{ad} , is defined as the temperature difference between saturation and condensation measured on an isentrope.

††† These calibrations were recomputed since they had been carried out for $\gamma = 1.67$ rather than $\gamma = 1.40$ (see references in the footnote on p.3). The effective area ratio at the exit determined from the present calibration with N_2 agreed with the previous calibration within 5% at $p_0 = 100$ torr and 1.5% at $p_0 = 800$ torr.

10 to 11°C for the 4 experiments evaluated. Clearly these results are no better than the initial estimates of the onset state and we conclude $\Delta T_{ad} = 10^\circ\text{C}$.

b) Discussion of Results

The following discussion has two aims. For one, we shall view our nitrogen experiment in the context of previous work. On the other hand, the experiments possibly to be pursued in the future will be subject to the same methods to be discussed here. Essentially similar work in a much extended range and with high accuracy can be expected. At first some remarks on the determination of the onset of condensation by light scattering.[†] No quantitative I_{90}/I_0 calibration was carried out. Owing to careful masking, use of a dark room and application of optical black on many components, the background light was minimal. Incipient condensation led to a large increase in the Rayleigh light scattering signal. The photomultiplier tube used, the tube voltage, the light scattering geometry, the He/Cd laser, and the thermodynamic state at the nozzle exit were all in a range similar to that of several previous investigations. Consequently we expect the measured increase of the scattered light to reflect clustering with concentrations of the order of 10^{11} clusters/cm³ with corresponding droplet radii of the order of 15 to 20 Ångstroms. The mass fraction condensed at that location is not

[†] This discussion leaves out the unknown exact state as caused by the absence of a "cold" nozzle calibration. (See Tables 2 and 3 and Figure 7).

readily determined, in fact this is the type of result which can later be estimated more accurately. However, with the above assumption and a typical density value (e.g. Exp. #32, Yale, Table 4) at the nozzle exit, the mass fraction of condensate, g , that can be detected is estimated to be $10^{-6} < g < 10^{-5}$. This value is at least two orders of magnitude lower than could be observed by a deviation of pressure from an isentropic expansion. As stated before, we may therefore find more realistic values for the adiabatic supercooling than noted in the past with a corresponding lower value seen by us.

It is thought, however, that the adiabatic supercooling may be slightly larger than shown in Table 4. This is a consequence of the fact that the boundary displacement thickness of the cooled nozzle may be somewhat lower than the one predicted by the mean values of Table 4 as shown in Figure 7. It is further interesting to note that the supercooling of Table 4 roughly agrees with that found at our laboratory in 1978 for pure argon using a similar apparatus. The surface tension of liquid argon ($T = -188\text{C}$, $\sigma = 13 \text{ erg/cm}^2$) is in fact not too different from that of liquid nitrogen ($T = -203\text{C}$, $\sigma = 11 \text{ erg/cm}^2$). The vapor pressures and indices of refraction are not too different. Consequently onset conditions of condensation may not be too different yielding similar differential cross sections.

These thoughts finally bring us to a comparison of our results — always based on the mean value as indicated by the dashed line in Figure 7 or the sample values of Table 4 — with previous work. In Figure 1 taken from the Proposal we show nozzle and free jet data. The nozzle

data refer to the work at the Cal. Inst. of Tech. in 1952 (Arthur, Buhler, Willmarth and Nagamatsu, see Proposal) and the work of the Applied Physics Lab. of JHU in 1952 (Faro et al., see Proposal). The free jet data came from recent (1978) German experiments (Dankert and Koppenwallner, see Proposal). The curve marked "Goglia" in Figure 7 represents his interpolation of his data and those of the CalTech group. However, the Goglia data[†] at low Mach numbers but higher pressures are most suitable for comparison with our results. We note that for condensation onset pressures below about 200 torr - roughly where the word *mean* appears in Figure 7 - Goglia connects his data points with those of the CalTech group. Shifting our mean curve slightly to the left, i.e., the cold nozzle side we find that an extension to higher pressures shows reasonable agreement of our data with Goglia's values. In fact an estimate of the adiabatic supercooling based on three of Goglia's experiments at higher pressures and temperatures given in Table 4 shows roughly the same adiabatic supercooling that we found. This comparison brings us to the final discussion of the cooling rate the second empirical parameter next to pressure level, that governs the adiabatic supercooling.^{††}

In general we have drastically different cooling rates for different experimental methods of study of nucleation. The expected ranges are roughly as follows:

† In addition to the readily accessible reference given in point (1) of Table 5 note: Gennaro Louis Goglia, "Limit of supersaturation of nitrogen vapor expanding in a nozzle," Doctoral Dissertation, University of Michigan 1959.

†† We use the adiabatic supercooling since small errors in pressure measurement cause large errors in the calculation of the supersaturation.

<u>Method</u>	<u>Estimated Cooling Rate Range (C/μs)</u>
atmospheric motion	10^{-10} to 10^{-7}
diffusion cloud chamber	10^{-8} to 10^{-7}
piston cloud chamber	10^{-7} to 10^{-5}
shock tube (expansion fan)	10^{-4} to 10^{-1}
wind tunnel [†]	10^{-2} to 10^1
shock tube (tailored interface)	$\sim 10^0$
molecular beam	10^2 to 10^4

In this list we note the extreme rates of cooling in free jets of molecular beams, consequently large supercooling is expected as observed in Figure 1. The shaded range in Figure 1 and 7 includes the results of the diverse sources mentioned. Most of the data were taken in hypersonic tunnels hence the overlap of Goglia's extrapolation at lower pressures. Our wind tunnel experiments were in contrast performed at cooling rates of about 0.10 C/μs as computed in Table 4 for four experiments. We see in the table that saturation takes place at $M \approx 2$, hence with condensation at $M \approx 2.6$, a lower cooling rate arises. It is this feature of the precooled, low Mach number experimental apparatus that can be varied to produce a wide range of cooling rates applicable to the flow fields about models in the transonic facility. Goglia's cooling rates, also estimated from his data in Table 4 are about twice ours. In line with

† Supply to test section, includes hypersonic tunnels.

past experience, a factor of two of this variable is not too important; thus no significant effect on the adiabatic supercooling arises between the two series of experiments. However, more accurate and extended experiments are clearly needed. In sum, our condensation data

provide results of interest in the lower pressure range of the

transonic facility,

have detected the onset of condensation at much smaller mass

fractions than noted previously, and

demonstrated that an extension of the techniques used could

cover the entire range noted in Figure 1 including a

substantial variation of the cooling rate.

3) STUDY OF PROPOSED CONDENSATION EXPERIMENTS.

A study is proposed to be carried out at Yale University where nitrogen expansions of the NASA Langley National Transonic Facility shall be duplicated in a small continuously operating wind tunnel covering a small fraction of the cross-sectional area of the prototype. Experiments are to be performed covering the range of supply states, Mach numbers and cooling rates around models of the full scale transonic tunnel to observe if supersaturation of the nitrogen can conservatively be expected. Preliminary experiments of this kind carried out with similar equipment were described in the previous Section 2 of this Final Report.

It is proposed to vary the conditions important to condensation in these experiments, by again (TABLE 6) varying the test gases at first from

ultrapurified nitrogen to prepurified nitrogen.[†] In addition it will be important to add systematic studies involving binary and heterogeneous nucleation. In such experiments small metered amounts of H₂O and/or aerosols of known geometry will be added to the nitrogen. In all cases the supply section, however, will have pure vapors (no droplets!) present.[†]

The proposed test facility will be instrumented by a combination of pressure measurements, Rayleigh light scattering experiments (light beams across the flow and on the centerline), schlieren photography and possibly interferometry.^{††} The experimental results will be compared with predictions of condensation based on solutions of the equations of motion in conjunction with the theory of nucleation and appropriate droplet growth laws.

The System

A wind tunnel of the kind shown in Figure 2 would be designed and constructed. Its basic features are discussed in Section 2 and the references given therein. The maximum size of the tunnel is limited by the capacity of our two existing Stokes Microvac Model 412-H pumps operating in parallel.^{†††} Their joint capacity for $0.01 < p_{\text{intake}} < 1 \text{ atm}$ is $2 \times 270 \text{ CFM} = 540 \text{ CFM} = 0.25 \text{ m}^3/\text{s}$. Assuming a range of initial conditions in the nozzle supply as shown by two limiting isentropes in Figure 1, the

† No significant differences are to be expected between both purified test gases as noted before in previous investigations of similar problems. See footnotes on p.3, also Wegener et al., Phys. Fluids 15, 1869 (1972) and Wegener and Wu, Faraday Discussion of the Chemical Soc., No. 61 (1976) in which binary nucleation experiments in supersonic flow are discussed.

†† We will consider the use of our Zeiss Mach-Zehnder Interferometer.

††† The capacity of our vacuum system can, of course, be increased by additional pumps if desirable.

data of TABLE 6 were computed. Here it is conservatively assumed that the throat area equals 1 cm^2 and that the pump intake pressure equals the test section pressure while the gas is isobarically heated to room temperature in the return pipes leading to the vacuum pumps below the floor of the laboratory. In other words we assume no pressure recovery in a diffuser. Note that the proposed tunnel is appreciably larger (compare Figure 5) than that used in the experiments described in Section 3. The estimated N_2 gas consumption and its cost is also shown in TABLE 6.^{††} A single experiment, i.e. the accurate determination of one point of incipient condensation in a $p(T)$ -diagram such as that shown in Figure 7, takes no more than about five minutes running time.^{††}

The N_2 gas is precooled in a liquid nitrogen heat exchanger similar to the one currently in use (see bottom of Figure 3). However, the gas flow will be divided into a number of different copper coils (3 or 4) whose discharge rate may be controlled independently. Moreover an additional gas feedline by-passes the heat exchanger, and all flows are mixed before entry into the tunnel supply. This mixing takes place in an insulated length of pipe between heat exchanger and tunnel supply computed for full mixing by turbulent pipe flow. In this fashion it will be possible to control the supply temperature of the wind tunnel in a wide range as needed to cover the demanded isentropes. Heat transfer calculations based on existing property data and appropriate values of heat transfer coefficients, thermal conductivity, etc. reveal a required total length, L , of

† The cost figures are subject to price escalation.

†† It is expected that reliable experiments can be performed at $A^* < L \text{ cm}^2$. Recall that \dot{m} and consequently cost are linear functions of the throat area. It may well be desirable to build a second nozzle with a smaller throat for the high pressure isentrope studies.

copper tubing (ID \approx 1 cm), fully immersed in an insulated box filled with liquid nitrogen at atmospheric pressure ($\sim 77^\circ\text{K}$), of approximately $5 < L < 8\text{m}$. The total length depends on supply conditions and the choice of separately operable coils and a by-pass will permit adjustment to a given supply temperature. These values are in line with our past experience (See Section 3).[†]

A number of substantial differences in design of the test section in comparison with the existing system (Figures 2 to 4) will be made. For one, the supply section will contain a fixed thermocouple rake to avoid surveying the supply temperature uniformity with a moveable thermocouple. Windows to observe the prescribed absence of condensation determined from light scattering in the supply will be available. All windows will be connected to the supply and test sections by evacuated chambers in order to avoid fogging. The entire supply section will again be double-walled to be cooled with liquid N_2 before and during actual tunnel operation. The nozzle will be of the type shown in Figure 5 with a continuous expansion. A cubic throat curve will be joined to a plane diverging wall to achieve a continuous second derivative of the surface to insure a smooth turbulent boundary layer growth. The nozzle will be equipped with static pressure taps to calibrate the flow without resorting to a nozzle calibration in a separate setup outside the cooled test section as done in the past. This calibration will be monitored at all operating conditions. The nozzle exit will extend into a large chamber. That chamber will have circular windows on all sides far removed from the jet to observe the jet visually and by the

[†] In fact the practical difficulty in the operation of such heat exchangers (or precoolers) lies in achieving temperatures appreciably above those of liquid nitrogen at its boiling point.

optical techniques mentioned before.[†] In this fashion fogging and other low temperature problems can be minimized. Moreover a number of fiber optic channels will be incorporated in the test section for attachment of photomultipliers on the outside at room temperature. In this fashion the onset of light scattering in the nozzle itself can be monitored. Currently this point was shifted to the nozzle exit by manipulation of the supply state. A more powerful blue laser than used in the previous work would also be useful (e.g. Liconix Helium Cadmium Laser Model 4050 giving 40 mW minimum at 442 nm).

The Flow

For the system described and the supply conditions of TABLE 6, the Reynolds numbers per unit length at $M = 2$ in the free stream will have the approximate range of $10^4 < Re/l < 5 \times 10^5 \text{ m}^{-1}$. Estimates of the displacement thickness of turbulent boundary layers at these conditions at a typical location about 10 cm from the throat lead to effective cross-sectional areas roughly 95% to 98% of the geometrical area for $M \approx 1.4$. This is a more favorable result than found from the calibration with a "warm" tunnel shown in Figure 6. At any rate, for each condensation experiment a calibration of the nozzle at identical supply conditions will be performed.

Finally, the cooling rate must be discussed. For simplicity, and in contrast to the results of TABLE 4 with saturation achieved at $M > 1$ (see Figure 7), we choose the throat region at that part of the nozzle giving the highest cooling rate.

[†] The laboratory permits operation in total darkness.

At the nozzle throat[†] denoted by an asterisk we have

$$\left[\frac{d(T/T_0)}{dt} \right]^* = - (R^* h^*)^{-1/2} \frac{(\gamma-1) a_0}{[(\gamma+1)/2]^2} ,$$

with

R^* radius of curvature at the nozzle throat,

h^* height of throat,

a_0 supply sound speed, and

γ ratio of the specific heats.

For nitrogen and with $\gamma = 1.40$, the above equation may be simplified to give

$$(dT/dt)^* = - (R^* h^*)^{-1/2} T_0^{3/2} 5.67 \text{ (}^\circ\text{C/s)} ,$$

with T_0 in K and the length R^* and h^* in meters.

For convenience we can approximate the throat and the following geometrical expansion in the nozzle by an arc. Using the equations given we can use typical throat radii (e.g. $R^* = 1$ m), nozzle lengths and nozzle heights compatible with the system described before. Cooling rates near the throat of $0.01 < -dT/dt < 0.1$ $^\circ\text{C/s}$ can be achieved. These values are even lower than those shown in TABLE 4 for the preliminary experiments. As one example we choose a nozzle with $R^* = 1$ m and $h^* = 10^{-2}$ m (for a 1 cm^2 throat area), and we assume $T_0 = 100$ $^\circ\text{K}$. Our equation gives $-dT/dt \approx 0.06$ $^\circ\text{C/s}$.

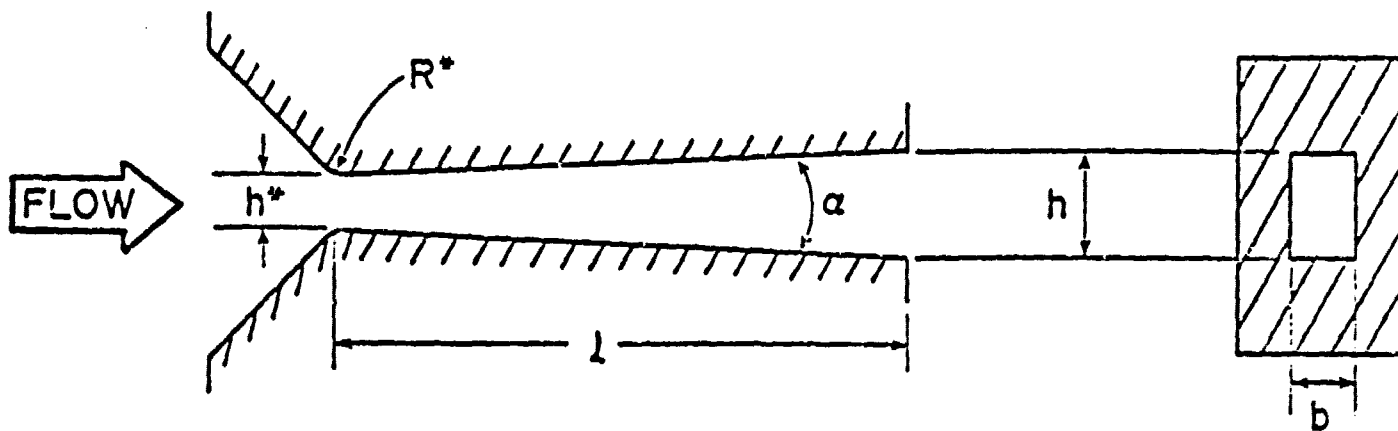
[†] See p. 707, Peter P. Wegener "CONDENSATION PHENOMENA IN NOZZLES", Progress in Astronautics and Aeronautics, pp. 701-724, Academic Press, Inc., New York (1964).

4) ACKNOWLEDGMENT

The preliminary experiments on the condensation of pure nitrogen given in this Final Report on Grant No. NSG-1612 would have been impossible without the cooperation of Dr. Benjamin J.C. Wu of the Brookhaven National Laboratory and Dr. Gilbert D. Stein of Northwestern University. Moreover, many of the ideas that could be utilized for a more extensive study were suggested by these two consultants. Mr. Jian Hsu of Yale University performed the calculations on the design of a wind tunnel facility in which condensation studies at Yale could be done on a more extensive scale. Mr. Carl Gandarillas, formerly of Yale University, performed the calculations on real gas effects described in the Appendix. The latter two also participated during the experiments and preparation.

Finally, during the work continuous contact was maintained with Dr. Robert M. Hall of the NASA-Langley Laboratory in order to adjust our procedures to the interests in line with the needs for the Transonic Facility. Moreover, Dr. Hall made many useful suggestions in the course of the study.

PRECEDING PAGE BLANK NOT FILMED



Nozzle	b (cm)	h* (cm)	A* (cm ²)	R* (cm)	h (cm)	l (cm)	alpha (deg)
A	1.16	1.10	1.28	3.4	1.54	5.7	4.4
B	0.70	0.40	0.28	2.	1.33	8.0	6.8
D	2.0	0.28	0.56	?	0.93	8.0	4.7

EXIT CONDITIONS		
Geometrical		
A/A*	M γ=1.67	M γ=1.4
1.40	1.86	1.76
3.33	3.16	2.75
3.32	3.16	2.74

TABLE 1: Geometry of various nozzles used in condensation experiments at Yale. Nozzle B used for pure nitrogen condensation experiments reported here. Similar nozzles would be proposed for extensive studies.

(1) Expt. #	(2) P_0 (torr)	(3) T_0 (C)	(4) T_0 (K)	(5) P_e/P_0 ← "hot" →	(6) P_e (torr)	(7) T_e (K) ← geometry →	(8) P_e (torr)	(9) T_e (K)	(10) M_e hot
2	463	-160	113	0.0574	27	49.9	18.4	45.4	2.513
6	244	-166	107	0.0655	16	49.1	9.7	42.6	2.428
9	244	-166	107	0.0655	16	49.1	9.7	42.6	2.428
11	338	-163	110	0.0608	20.6	49.4	13.4	43.8	2.476
12	405	-162	111	0.0588	23.8	49.4	16.1	44.2	2.497
13	409	-162	111	0.0587	24.0	49.4	16.3	44.2	2.498
20	671	-151	122	0.0540	36.2	53.0	26.7	48.6	2.552
22	468	-157	116	0.0573	26.8	51.2	18.6	46.2	2.514
23	502	-157	116	0.0566	28.4	51.1	23.0	46.2	2.522
27	710	-155	118	0.0539	38.3	51.2	28.2	47.0	2.553
28	973	-149	124	0.0535	52.1	53.7	38.7	49.4	2.558
29	744	-152	121	0.0537	40.0	52.5	29.6	48.2	2.555
30	893	-151	122	0.0536	47.9	52.9	35.5	48.6	2.557
31	871	-152	121	0.0536	46.7	52.4	34.6	48.2	2.557
32	1150	-144	129	0.0535	61.5	55.9	45.7	51.3	2.558
37	1209	-141	132	0.0535	64.7	57.2	48.1	52.5	2.558
40	1357	-139	134	0.0535	72.6	58.0	54.0	53.3	2.558

TABLE 2: Raw data and derived data of pure N₂ condensation experiments taken in Nozzle B (TABLE 1) performed on the NASA-Langley contract. For legend see TABLE 3. For all experiments listed condensation was observed to appear at the exit of NOZZLE B. At this location the Mach number for inviscid flow is $M_e = 2.75$. Table values of derived quantities were calculated to three place accuracy in P_e/P_0 and four place accuracy for M_e . Actual values are known to one less place only.

TABLE 3:
Legend for TABLE 2. †

- (1) Number of experiment.
- (2) Supply pressure, p_o .
- (3). (4) Supply temperature, T_o .
- (5) p_e refers to pressure at the exit of the nozzle ($l=8$ cm, TABLE 1). p_e/p_o as shown was measured for pure nitrogen (no condensation) as a function of p_o at a supply temperature of roughly 290 K (see Figure 1). These are the values given in column (5). Boundary layer effects for this "hot" case - (compare T_o -values of columns (3) and (4) - lead to effective nozzle exit area ratios (see Figure 1) that are smaller than those of the low temperature case. For low T_o -values no calibration exists.
- (6) p_e found by multiplying values of columns (2) and (3).
- (7) T_e , estimated exit temperature, found from $T_e = T_o (p_e/p_o)^{(\gamma-1)/\gamma}$ with T_o from column (3) and p_e/p_o from column (5) with $\gamma = 1.4$. ††
The values in columns (6) and (7) give one limiting condition of the thermodynamic state of expected condensation onset on the isentrope.
- (8) p_e computed for inviscid flow. From TABLE 1 we find the exit Mach number of Nozzle B as $M = 2.75$. Consequently $p_e/p_o = 0.0398$ for $\gamma = 1.4$. Multiplying this fixed value with those of column (2) gives the values of column (8).
- (9) T_e computed like the T_e of column (7), however with fixed $p_e/p_o = 0.0398$. Columns (8) and (9) consequently give a second limit for the condensation onset conditions on an isentrope, the zero boundary layer limit.
- (10) M_e derived from column (5). The corresponding Mach number for inviscid flow as derived from the area ratio is given by $M_e = 2.75$.

† Condensation results of TABLE 2 are shown in Figure 7.

†† It was separately shown that the flow can be treated as that of a calorically and thermally perfect gas.

(1) Expt. #	Saturation				Onset: (mean)				(8) \bar{u} (m/s)	(9) ΔT_{ad} (C)	(10) $-\frac{dT}{dt}$ °C/ μ s
	(2) p (torr)	(3) T (K)	(4) M	(5) p (torr)	(6) T (K)	(7) M					
11 Yale	38	59	2.08	16	48	2.56	337	11	0.10		
20 Yale	60	61	2.23	30	50	2.67	365	11	0.09		
27 Yale	78	62	2.10	41	52	2.51	348	10	0.11		
32 Yale	96	63	2.27	52	53	2.67	377	10	0.09		

140-6 Goglia $P_o = 10.6$ atm	470	74	2.49	314	65	2.75	446	9	0.21		
180-2 Goglia $P_o = 13.2$ atm	340	71	2.87	195	61	3.25	496	10	0.19		
180-6 Goglia $P_o = 13.2$ atm	340	71	2.87	201	61	3.23	496	10	0.21		

TABLE 4: Thermodynamic state at saturation and mean values at the onset of condensation for sample experiments of this work and that of G.L. Goglia.

TABLE 5:

Legend for TABLE 4.

- (1) Number of experiment. For supply state, etc. see TABLE 2 for the Yale experiments. For the Goglia experiments see e.g. G.L. Goglia and G.J. Van Wylen, Trans. ASME 83, Ser.C, 27, (J. Heat Transfer), 1961.
- (2), (3), (4) Thermodynamic state at saturation based on $p_{\infty}(T)$ of NBS, Circular 564, (1955).
- (5), (6), (7) Thermodynamic state at the onset of condensation. Mean value of states for inviscid flow and "hot" calibration (see TABLE 3).
- (8) Average flow speed between saturation and the onset of condensation \bar{u} (m/s).
- (9) Adiabatic supercooling ΔT_{ad} (C), i.e. temperature difference between saturation and condensation onset.
- (10) Average cooling rate dT/dt (C/ μ s) computed by dividing ΔT_{ad} by the time of motion of a fluid element at speed \bar{u} (8) between the location of saturation in the nozzle and the nozzle exit. Note that condensation is forced to appear at the nozzle exit.

LIQUID N₂

GAS N₂

P ₀ atm	T ₀ K	\dot{m} kg/s	cost \$/min		\dot{m} kg/min	cost \$/min
			† pp	†† upp		
0.5	77	0.023	4	12	1.4	2
1.0	83	0.044	8	23	2.6	3.6
3.0	94	0.12	22	64	6.9	9.8
5.0	100	0.20	35	103	11	15
7.0	104	0.28	68	142	15	21
9.0	107	0.35	61	180	19	27

† prepurified, 99.998% (Fall 1979 prices)

†† ultra high purity, 99.999% (Fall 1979 prices)

TABLE 6: Consumption rates of a wind tunnel operated with N₂ with a throat area of 1 cm² in the range of isentropes of Figure 1. Discharge rates of N₂ (m) at the supply conditions indicated and use of liquid N₂ to precool the gas to the supply state are shown. Note additional cost estimates.

NITROGEN CONDENSATION

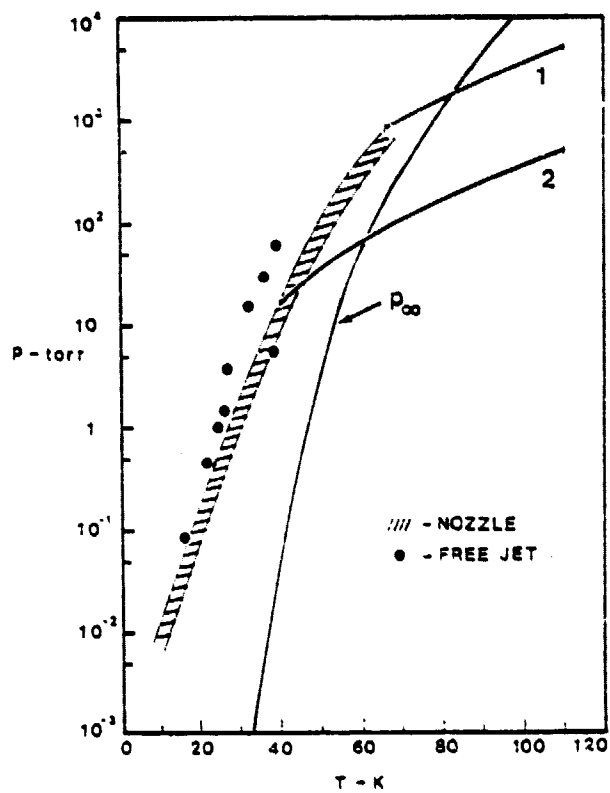


FIGURE 1: Results on pure N_2 condensation in nozzles and free jets from several sources (see proposal). Isentropes 1 and 2 bracket the conditions for operation of the National Transonic Facility.

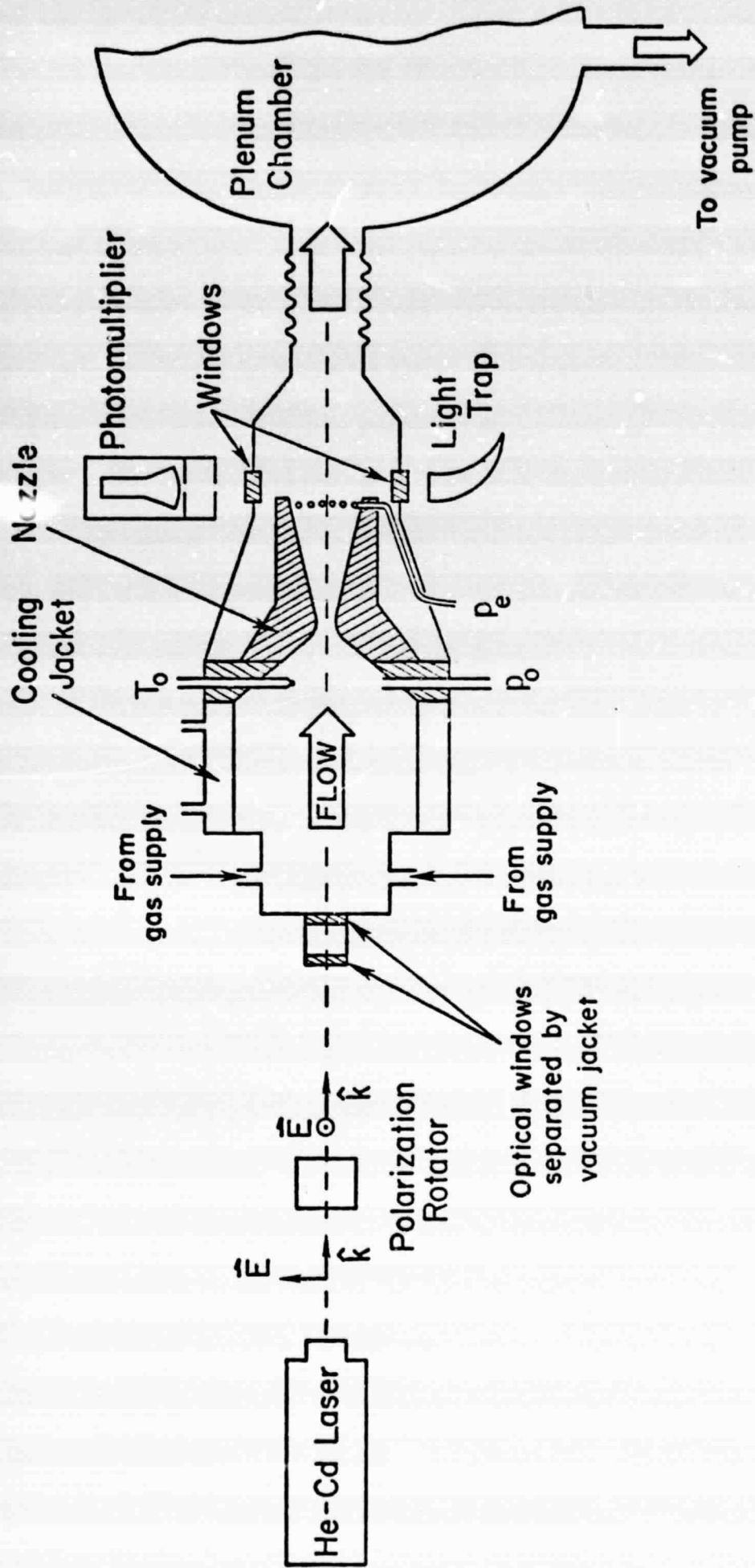


FIGURE 2: Schematic drawing of the experimental setup used to study N_2 condensation. A similar arrangement would be proposed for an intensive study.

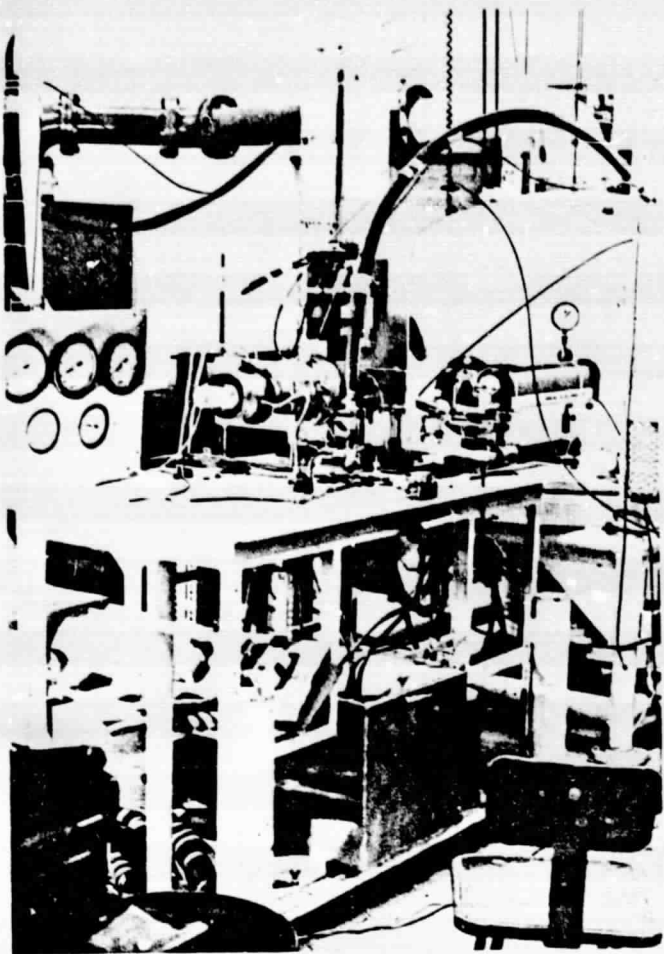


FIGURE 3: Wind tunnel (flow from left to right) and plenum chamber. Note liquid N₂ cooler at bottom.

ORIGINAL PAGE IS
OF POOR QUALITY

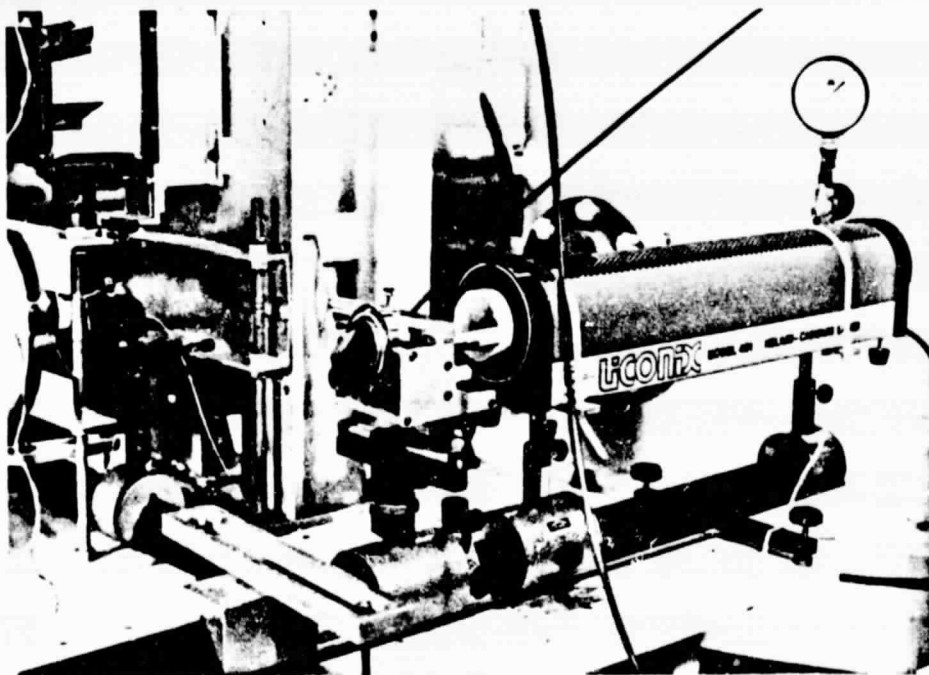


FIGURE 4:

He-Cd laser (blue) and optical arrangement to determine light scattering at nozzle exit.

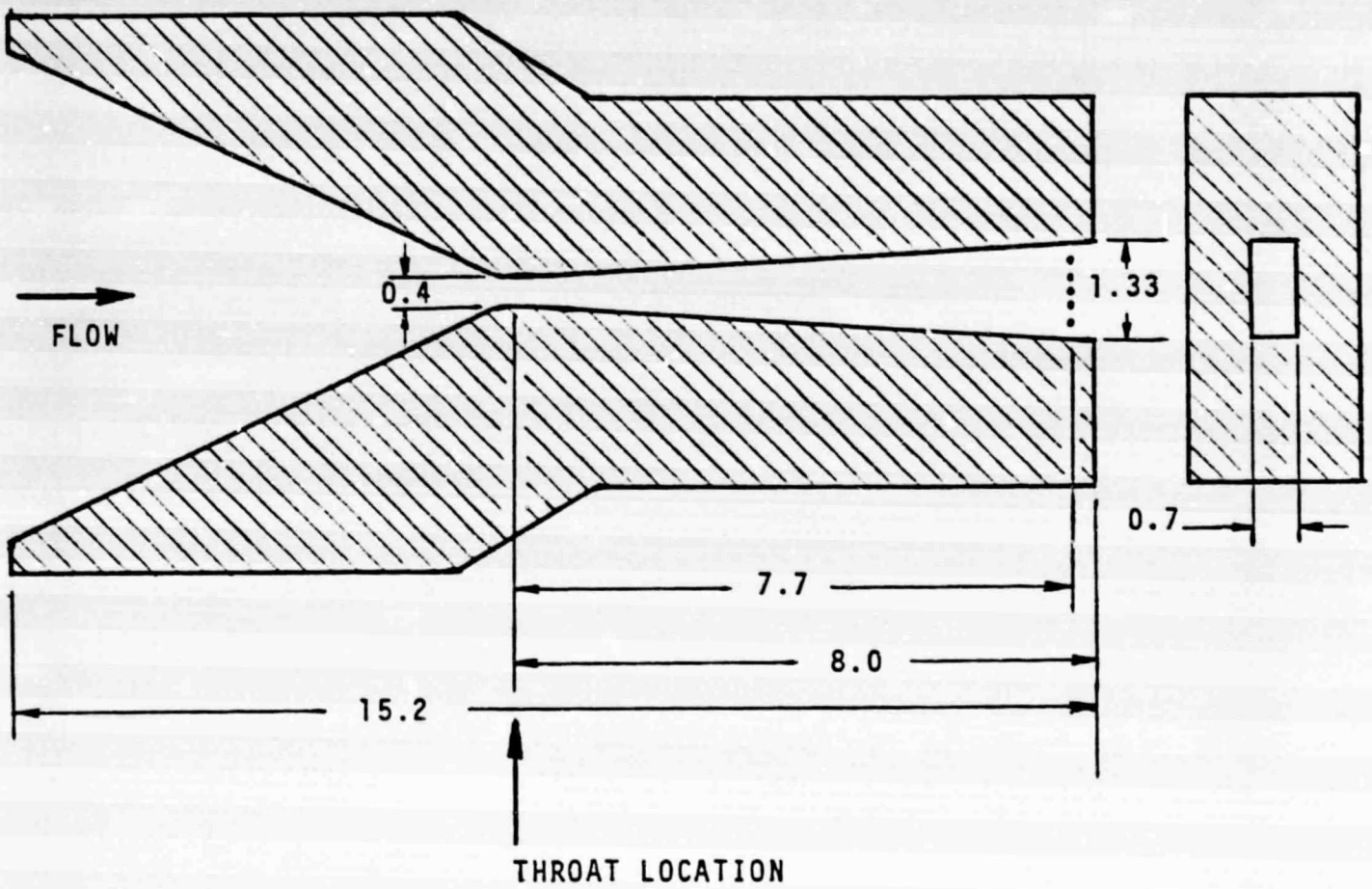


FIGURE 5: Nozzle B (also note Table 1); Full scale.
 $A/A^* = 3.3$ at nozzle exit. All dimensions
 in centimeters.

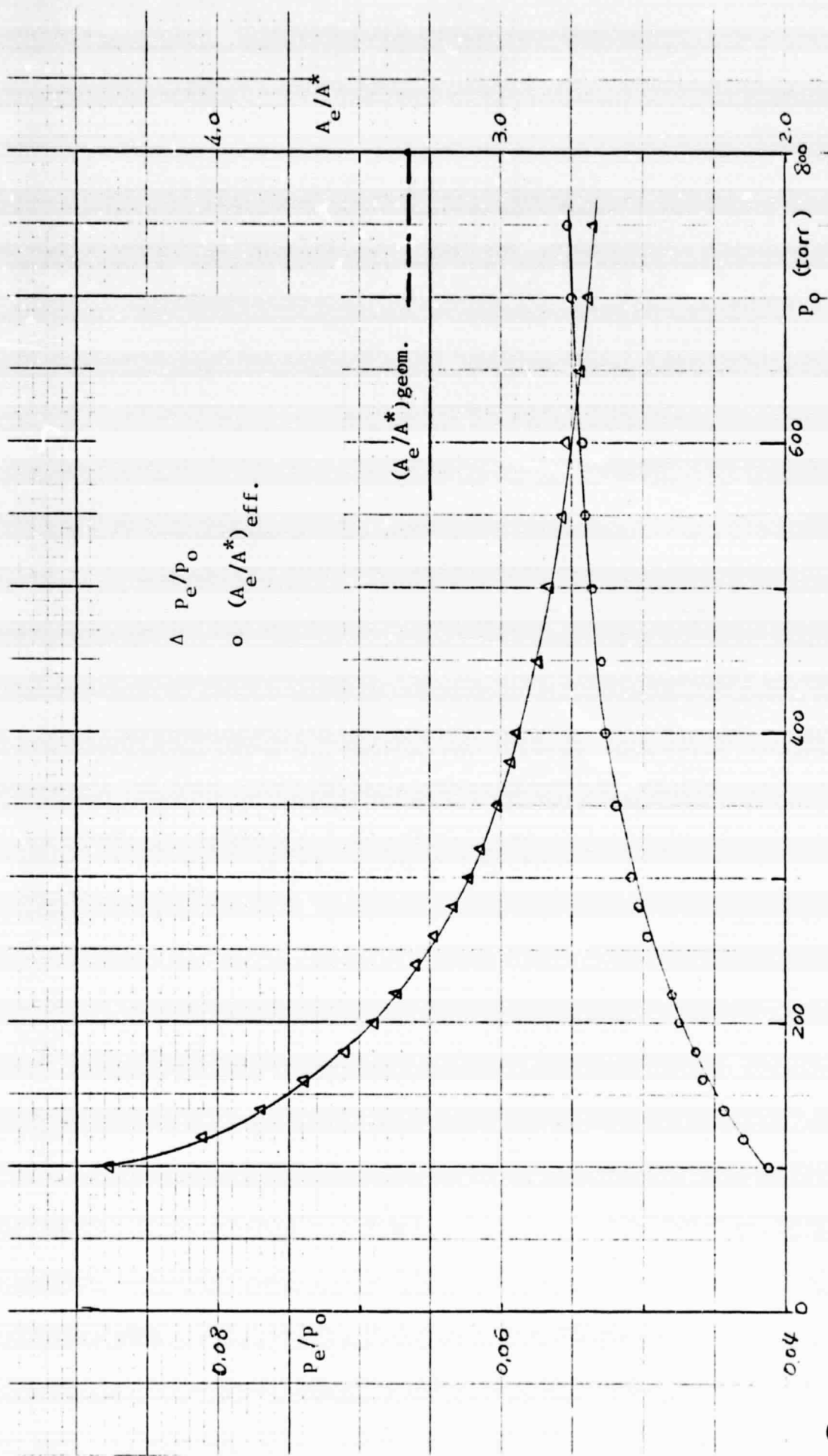


FIGURE 6: Calibration of Nozzle B (TABLE 1 and Figure 5) with dry nitrogen. Measured static pressure at the exit of the nozzle, P_e , as a function of supply pressure and computed effective area ratios for $\gamma = 1.40$. (Supply temperature = room temperature).

ORIGINAL PAGE IS
 OF POOR QUALITY

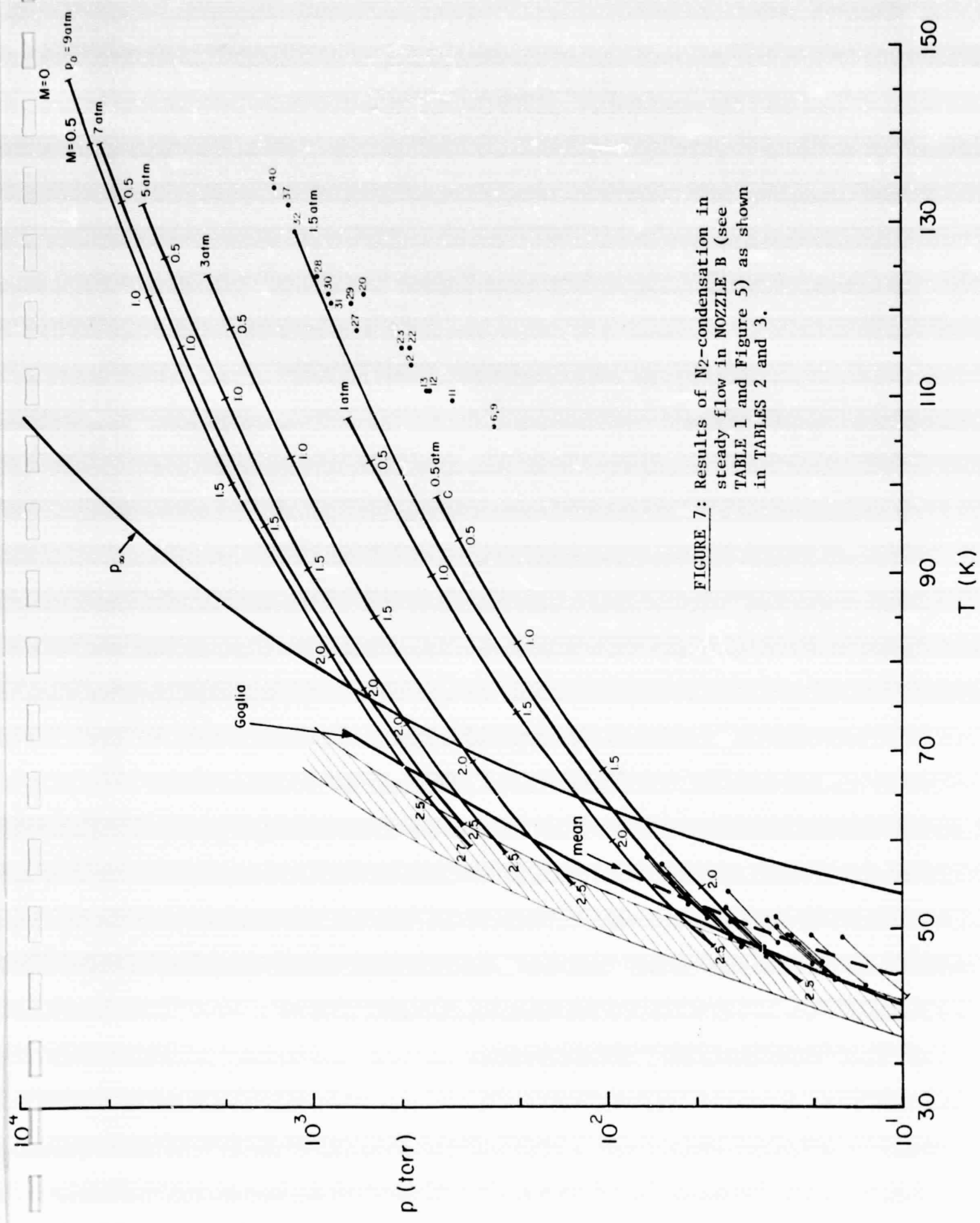


FIGURE 7: Results of N_2 -condensation in steady flow in NOZZLE B (see TABLE 1 and Figure 5) as shown in TABLES 2 and 3.

APPENDIX: Isentropic Expansion of Nitrogen using Berthelot's
Equation of State.

List of Symbols

A	area
c	constant
c_p	specific heat at constant pressure
c_{po}	ideal gas (thermally ideal) specific heat, Eq. (9)
h	enthalpy
h_o	enthalpy at reservoir conditions
p	pressure
p_c	critical pressure
ρ	density
R	gas constant
s	entropy
T	temperature
T_c	critical temperature
u	flow speed
v	specific volume
x	distance

Summary

The steady, one-dimensional, isentropic expansion of nitrogen is formulated using the equation of state suggested by Berthelot. The gasdynamic variables for supersonic nozzle flow are calculated assuming that no condensation takes place even though the nitrogen may be in supersaturated states. The results show the Berthelot gas model to be close to (less than 0.2% deviation) both the real gas calculations of Adcock (Ref. 1) and the ideal gas calculations. Therefore, the ideal gas equation may be used with sufficient accuracy in the temperature and pressure range of interest.

Derivation

The conservation equations of steady state, one-dimensional, inviscid nozzle flow take the form:

$$\text{continuity: } \rho Au = \dot{m} = \text{constant.} \quad (1)$$

$$\text{momentum: } u \frac{du}{dx} + \frac{1}{\rho} \frac{dp}{dx} = 0. \quad (2)$$

$$\text{energy: } \frac{1}{2} u^2 + h = h_0 = \text{constant.} \quad (3)$$

Combining Eq. (2) and the differential form of Eq. (3) gives

$$\frac{1}{\rho} dp = dh, \quad (4)$$

which implies $ds = 0$ by virtue of the thermodynamic relation

$$dh = Tds + \frac{1}{\rho} dp. \quad (5)$$

Hence, the momentum equation may be replaced by the isentropic conditions:

$$s = s_0 = \text{constant}. \quad (6)$$

Thus, the solution of the set of equations (1), (3), and (6) requires expressions for the enthalpy, $h(p,T)$, the entropy, $s(p,T)$, and the thermal equation of state, $\rho(p,T)$. In fact, the ideal gas specific heat $c_{p0}(T)$, and $\rho(p,T)$ are all that is needed to generate the functions $h(p,T)$ and $s(p,T)$.

The Berthelot Thermal Equation of State* can be written

$$pv = RT \left[1 + \frac{9}{128} \left(\frac{pT_c}{p_c T} \right) \left(1 - \frac{6T_c^2}{T^2} \right) \right], \quad (7)$$

where the subscript c denotes the critical properties. For nitrogen we have

$$T_c = 126.2 \text{ }^\circ\text{K}, \text{ and } p_c = 33.5 \text{ atm.}$$

Thus, Eq. (7) can be written as

$$v = \frac{RT}{p} + c_1 R \left(1 - \frac{c_2}{T^2} \right), \quad (8)$$

* Ref. 3, p. 296.

where

$$c_1 = \frac{9}{128} \frac{T_c}{p_c} = 3.485 \times 10^{-4} \frac{^\circ\text{K}}{\text{mm Hg}},$$

$$c_2 = 6 T_c^2 = 9.556 \times 10^4 (^\circ\text{K}).$$

The ideal gas specific heat capacity at constant pressure, c_{po} is taken from Jacobsen (Ref.4) and it is expressed by

$$c_{po}(T) = R \sum_{i=1}^7 N_i T^{i-4}. \quad (9)$$

The 7 constants N_i in Eq. (9) are tabulated by Jacobsen based on experimental results. The results obtained with Eq. (9) are plotted in Fig. A1 in the form of a deviation of real from ideal heat capacity values given in percent. We note that for $30 < T < 130^\circ\text{K}$, nitrogen is essentially a calorically ideal gas. The ideal value of $c_{po}/R = 3.5$ is given by N_4 in Eq. (9).

Next the enthalpy and entropy are derived by following the procedure described in Ref. (2) on pp.10-32 to 10-39. The path of the integration shows 3 steps. The results are

$$h(p, t) = Kp \left(c_1 - \frac{3c_1c_2}{T^2} \right) + R \left[\sum_{\substack{i=1 \\ i \neq 3}}^7 N_i \frac{T^{i-3}}{(i-3)} + N_3 \ln(T) \right], \quad (10)$$

and

$$s(p,T) = - R \ln p + R \left[\sum_{\substack{i=1 \\ i \neq 4}}^7 \frac{T^{i-4}}{(i-4)} + N_4 \ln(T) \right] - 2Rc_1c_2 \left(\frac{p}{T^3} \right). \quad (11)$$

The speed of sound is required to determine the Mach number. In general for an equation of state $\rho = \rho(p,T)$, the speed of sound, c , is given by

$$c \equiv \sqrt{\left(\frac{\partial p}{\partial \rho} \right)_s}, \quad (12)$$

where

$$\left(\frac{\partial p}{\partial \rho} \right)_s = \left[\left(\frac{\partial p}{\partial p} \right)_T - \left(\frac{\partial p}{\partial T} \right)_p \left(\frac{\partial s}{\partial p} \right)_T \left(\frac{\partial s}{\partial T} \right)_p^{-1} \right]^{-1}. \quad (13)$$

For the Berthelot gas, the required derivatives in Eq. (13) are:

$$\left(\frac{\partial p}{\partial p} \right)_T = \frac{\rho^2 RT}{p^2}, \quad (14)$$

$$\left(\frac{\partial p}{\partial T} \right)_p = - \rho^2 R \left(\frac{1}{p} + \frac{2c_1c_2}{T^3} \right), \quad (15)$$

$$\left(\frac{\partial s}{\partial p} \right)_T = - R \left(\frac{1}{p} + \frac{2c_1c_2}{T^3} \right), \quad (16)$$

and

$$\left(\frac{\partial s}{\partial T} \right)_p = R \left[\sum_{i=1}^7 N_i T^{i-5} + 6c_1c_2 \frac{p}{T^4} \right]. \quad (17)$$

Finally the set of Eqs. (1), (3) and (6) can be solved using temperature as the independent variable. From a given initial state, (p_0, T_0) , the entropy of the system, s_0 , is calculated using Eq. (11). To find the pressure at any other temperature, T , Eq. (11) is solved by trial and error. Once the pressure has been found, the remaining variables are found in a straightforward way. The computer was used to facilitate these calculations.

The results are shown in Table A1. Less than 1% deviation in pressure and temperature from the ideal gas values are found over the range of interest, however, Adcock's real gas calculations (Ref. 1) also show less than 1% deviation from the ideal gas values. Hence, in the range of interest, the ideal gas equation may be used with sufficient accuracy. This result greatly simplifies the determination of the states of observed onset of condensation permitting the use of standard flow tables.

References for Appendix

1. Adcock, Jerry B., Real-Gas Effects Associated with One-Dimensional Transonic Flow of Cryogenic Nitrogen, NASA TN D-8274, Dec. 1976.
2. Cravalho, Ernest G. and Smith, Joseph L., Thermodynamics, Holt, Rinehart, and Winston, Inc., 1971.
3. Glasstone, Samuel, Textbook of Physical Chemistry, D. Van Nostrand Co., Inc., 1946.
4. Jacobsen, R.T. and Stewart, R.B., Thermophysical Properties of Nitrogen From the Fusion Line to 3500 R (1944 K) For Pressures to 150,000 psia ($10342 \times 10^5 \text{ N/m}^2$), NBS Technical Note 648, Dec. 1973.
5. Shapiro, Ascher H., The Dynamics and Thermodynamics of Compressible Fluid Flow, V.I., Ronald Press, N.Y., 1953.
6. Vargaftik, N.B., Tables on the Thermophysical Properties of Liquids and Gases, 2nd Ed., Hemisphere Publishing Corp., 1975.
7. Woolley, Harold W., Thermodynamic Properties of Gaseous Nitrogen, NACA TN 3271, March 1956.
8. Wu, Benjamin J.C., Evaluation of Recent SF₆ Condensation Experiments Including Specific Heat Variation, Report #4, Contract XP5-76557-1, Los Alamos-Yale, Nov. 30, 1976.

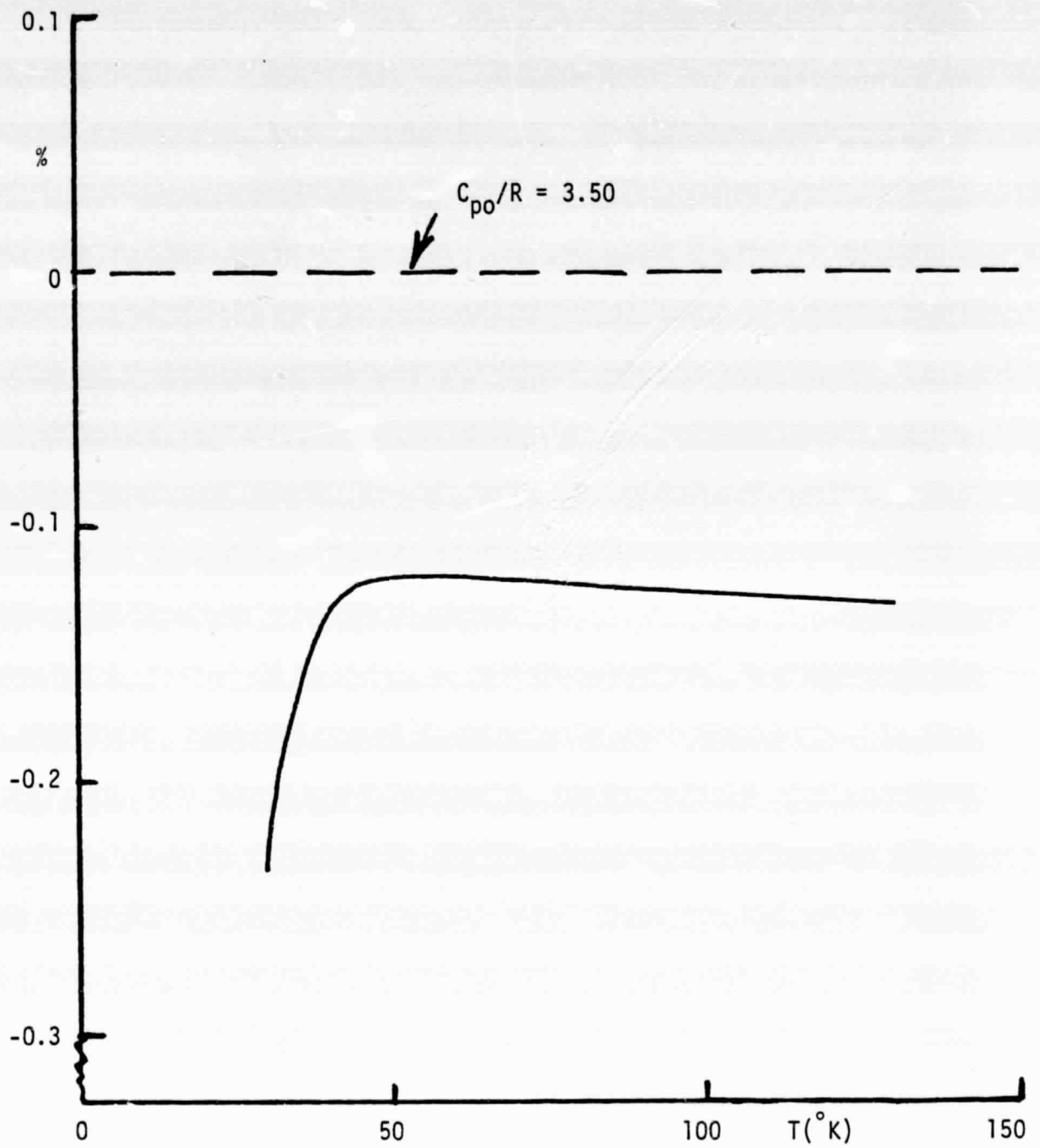


FIGURE A1: Deviation in % of the specific heat of nitrogen computed from Eq.(9) in relation to the ideal gas value.

BERTHELOT GAS ISENTROPIC EXPANSION OF NITROGEN.

PO = 2280.0 MMHG, TO = 90.0 K, VO = 79.49 CC/GM, SO = 0.5554 CAL/GM-K, HO = 20.2238 CAL/GM

Table with columns: MACH, REY/M, Z, C M/SEC, P/PO, T/TO, V/VO, H/HO, A/A#, C RELATIVE TO IDEAL, P/PO RELATIVE TO IDEAL, T/TO IDEAL, V/VO GAS VALUES, A/-. Contains numerical data for Mach 0.0 to 1.0.

Handwritten annotations: '3 atm' with an upward arrow, '4 atm' with a downward arrow, and '90K'.

BERTHELOT GAS ISENTROPIC EXPANSION OF NITROGEN.

PO = 3041.0 MMHG, TO = 90.0 K, VO = 57.52 CC/GM, SO = 0.5301 CAL/GM-K, HO = 14.5777 CAL/GM

Table with columns: MACH, REY/M, Z, C M/SEC, P/PO, T/TO, V/VO, H/HO, A/A#, C RELATIVE TO IDEAL, P/PO RELATIVE TO IDEAL, T/TO IDEAL, V/VO GAS VALUES, A/-. Contains numerical data for Mach 0.0 to 1.0.

BERTHELOT GAS ISENTROPIC EXPANSION OF NITROGEN.

PO = 5320.0 MMHG, TO = 90.0 K, VO = 29.28 CC/GM, SO = 0.4756 CAL/GM-K, HO = 17.6393 CAL/GM

Table with columns: MACH, REY/M, Z, C/M/SEC, P/P0, T/T0, V/V0, H/H0, A/A0, C, P/P0, T/T0, V/V0, A. Includes handwritten annotations: '7 atm' with an upward arrow and '8 atm' with a downward arrow.

↑ 7 atm

90K

↓ 8 atm

BERTHELOT GAS ISENTROPIC EXPANSION OF NITROGEN.

PO = 6000.0 MMHG, TO = 90.0 K, VO = 24.57 CC/GM, SO = 0.4512 CAL/GM-K, HO = 16.9932 CAL/GM

Table with columns: MACH, REY/M, Z, C/M/SEC, P/P0, T/T0, V/V0, H/H0, A/A0, C, P/P0, T/T0, V/V0, A. This table is a duplicate of the one above.

THELOT GAS ISENTROPIC EXPANSION OF NITROGEN.

=6840.0 MMHG, T0 = 90.0 K, V0 = 20.91 CC/GM, S0 = 0.4479 CAL/GM-K, H0 = 16.3471 CAL/GM

Table with columns: CH, P/ATM, FLY/M, Z, M/SEC, P/P0, T/T0, V/V0, H/H0, A/A#, C, P/P0, T/T0, V/V0, A/A#. Contains numerical data for gas expansion.

Handwritten annotations: ↑ 9 atm, 90K, ↓ 10 atm

THELOT GAS ISENTROPIC EXPANSION OF NITROGEN.

=7000.0 MMHG, T0 = 90.0 K, V0 = 17.98 CC/GM, S0 = 0.4355 CAL/GM-K, H0 = 15.7010 CAL/GM

Table with columns: CH, P/ATM, FLY/M, Z, M/SEC, P/P0, T/T0, V/V0, H/H0, A/A#, C, P/P0, T/T0, V/V0, A/A#. Contains numerical data for gas expansion.

HO4001 EXECUTION TERMINATING DUE TO ERROR COUNT FOR ERROR NUMBER 217

HO2171 FIDCS - END OF DATA SET ON UNIT 5

TRACEBACK ROUTINE CALLED FROM ISN REG. 14 REG. 15 REG. 0 REG. 1
IBCOM 00099D1C 00 8A4 0000002B 0009A02A
MAIN 0000H170 00000010 00000010 00094F98

ERTHELCT GAS ISENTROPIC EXPANSION OF NITROGEN.

3 ATM

0 = 2230.0 MMHG, T0 = 110.0 K, V0 = 102.04 CC/GM, S0 = 0.6119 CAL/GM-K, H0 = 25.8478 CAL/GM

Table with columns: MACH, FEY/M, Z, C M/SEC, P/P0, T/T0, V/V0, H/H0, A/A0, C, P/P0, T/T0, V/V0, A/A0. Includes handwritten annotations: '3 atm' with an upward arrow and '110K'.

↑ 3 atm

110K

↓ 4 atm

ERTHELCT GAS ISENTROPIC EXPANSION OF NITROGEN.

4 ATM

0 = 3040.0 MMHG, T0 = 110.0 K, V0 = 75.19 CC/GM, S0 = 0.5888 CAL/GM-K, H0 = 25.4215 CAL/GM

Table with columns: MACH, FEY/M, Z, C M/SEC, P/P0, T/T0, V/V0, H/H0, A/A0, C, P/P0, T/T0, V/V0, A/A0.

RHTELCT'S ISENTROPIC EXPANSION OF NITROGEN.

5 ATM

#300.0 MMHG, T0 = 110.0 K, V0 = 59.68 CC/GM, S0 = 0.5703 CAL/GM-K, H0 = 24.9952 CAL/GM

Table with columns: ACH, REY/M, Z, C M/SEC, P/P0, T/T0, V/V0, H/H0, A/A#, C, P/P0, T/T0, V/V0, A/A#. The table contains multiple columns of numerical data representing gas properties during isentropic expansion.

Handwritten annotations: '15 atm' with an upward arrow and '6 atm' with a downward arrow.

Handwritten annotation: '110K'

RHTELCT GAS ISENTROPIC EXPANSION OF NITROGEN.

6 ATM

#430.0 MMHG, T0 = 110.0 K, V0 = 48.35 CC/GM, S0 = 0.5546 CAL/GM-K, H0 = 24.5683 CAL/GM

Table with columns: ACH, REY/M, Z, C M/SEC, P/P0, T/T0, V/V0, H/H0, A/A#, C, P/P0, T/T0, V/V0, A/A#. The table contains multiple columns of numerical data representing gas properties during isentropic expansion.

ORIGINAL PAGE IS OF POOR QUALITY

WETHELDY'S ISENTROPIC EXPANSION OF NITROGEN.

7 ATM

C = 5330.0 MMHG, T0 = 110.0 K, V0 = 40.67 CC/GM, S0 = 0.5410 CAL/GM-K, H0 = 24.1425 CAL/GM

Table with columns: WACH, REY/M, Z, C (M/SEC), P/P0, T/T0, V/V0, H/H0, A/A0, C (RELATIVE TO IDEAL), P/P0, T/T0, V/V0, A/A0. Contains multiple columns of numerical data for nitrogen expansion at 7 atm.

↑ 7 atm

↓ 8 atm

110 K

8 ATM

WETHELDY'S ISENTROPIC EXPANSION OF NITROGEN.

C = 5330.0 MMHG, T0 = 110.0 K, V0 = 34.92 CC/GM, S0 = 0.5288 CAL/GM-K, H0 = 23.7162 CAL/GM

Table with columns: WACH, REY/M, Z, C (M/SEC), P/P0, T/T0, V/V0, H/H0, A/A0, C (RELATIVE TO IDEAL), P/P0, T/T0, V/V0, A/A0. Contains multiple columns of numerical data for nitrogen expansion at 8 atm.

